Mechanisms of deep brain stimulation: an intracellular study in rat thalamus

Trent Anderson, Bin Hu, Quentin Pittman and Zelma H. T. Kiss

Department of Clinical Neuroscience and Neuroscience Research Group, University of Calgary, Calgary, Alberta, Canada

High-frequency deep brain stimulation (DBS) in the thalamus alleviates most kinds of tremor, yet its mechanism of action is unknown. Studies in subthalamic nucleus and other brain sites have emphasized non-synaptic factors. To explore the mechanism underlying thalamic DBS, we simulated DBS *in vitro* by applying high-frequency (125 Hz) electrical stimulation directly into the sensorimotor thalamus of adult rat brain slices. Intracellular recordings revealed two distinct types of membrane responses, both of which were initiated with a depolarization and rapid spike firing. However, type 1 responses repolarized quickly and returned to quiescent baseline during simulated DBS whereas type 2 responses maintained the level of membrane depolarization, with or without spike firing. Individual thalamic neurones exhibited either type 1 or type 2 response but not both. In all neurones tested, simulated DBS-evoked membrane depolarization was reversibly eliminated by tetrodotoxin, glutamate receptor antagonists, and the Ca^{2+} channel antagonist Cd^{2+}. Simulated DBS also increased the excitability of thalamic cells in the presence of glutamate receptor blockade, although this non-synaptic effect induced no spontaneous firing such as that found in subthalamic nucleus neurones. Our data suggest that high-frequency stimulation when applied in the ventral thalamus can rapidly disrupt local synaptic function and neuronal firing thereby leading to a 'functional deafferentation' and/or 'functional inactivation'. These mechanisms, driven primarily by synaptic activation, help to explain the paradox that lesions, muscimol and DBS in thalamus all effectively stop tremor.

(Received 19 March 2004; accepted after revision 23 June 2004; first published online 24 June 2004)
Corresponding author Z. Kiss: 3330 Hospital Drive NW, Room 168 HMRB, Calgary, Alberta T2N 4N1, Canada. Email: zkiss@ucalgary.ca

High-frequency thalamic deep brain stimulation (DBS) delivered through a multipolar electrode implanted into the ventral-lateral (VL) thalamus alleviates parkinsonian, essential and cerebellar tremor (Schuurman *et al.* 2000). How such electrical stimulation can produce immediate and dramatic tremor suppression is unknown. Theoretical models indicate that the effect of DBS is primarily through the excitation of large-diameter axons, as they generally possess a lower threshold for excitation than cell somata (Ranck, 1975; Holsheimer *et al.* 2000; McIntyre & Grill, 2002). On the other hand, extracellular recordings from human thalamus following a high frequency DBS train show a more complex pattern of responses: excitation or inhibition, the latter of which is often preceded by burst firing (Dostrovsky *et al.* 2002). Furthermore, chemically induced thalamic neuronal inhibition by intranuclear injection of GABAergic receptor agonist, muscimol, appears equally effective in stopping tremor as DBS (Pahapill *et al.* 1999). How these clinical data can be reconciled and subsequently provide a scientific rationale for DBS therapy has become a current subject of intense debate (Windels *et al.* 2000; Dostrovsky *et al.* 2000; Perlmutter *et al.* 2002; Vitek, 2002; Anderson *et al.* 2003*a*; Hashimoto *et al.* 2003; Maurice *et al.* 2003; Sommer, 2003).

The portion of the VL thalamus that hosts the DBS electrode contains not only the somata of thalamocortical relay and interneurones, but also a vast number of axons and terminals that are predominantly glutamatergic and of cortical and cerebellar origin (Jones, 1985; Deschênes & Hu, 1990; Kiss *et al.* 2003*a*; Stepniewska *et al.* 2003). Prolonged high frequency (100–200 Hz) DBS may therefore exert its modulatory effects on multiple neural elements, disrupting abnormal rhythmic activities imposed by tremor cells (Kiss *et al.* 2002). Somewhat in contrast to this view, recent studies that utilize *in vitro* brain slices obtained from the hippocampus and subthalamic nucleus (STN) have found that persistent intranuclear stimulation alters neuronal firing rate independent of synaptic transmission. Simulated DBS (sDBS) in these structures suppresses a Na^+ membrane

© The Physiological Society 2004 DOI: 10.1113/jphysiol.2004.064998

conductance that is intrinsic to neuronal somata (Beurrier *et al.* 2001) and/or depolarizes neurones as a result of accumulation of external K^+ (Bikson *et al.* 2001; Lian *et al.* 2003). In this study we examined both the synaptic and non-synaptic mechanisms of sDBS in ventral-lateral (VL) and ventral-posterior (VP) thalamic slices obtained from adult rats. The predominant effect of intranuclear sDBS was membrane depolarization and disruption of thalamic neuronal activities by acting upon glutamatergic synaptic input (Anderson *et al.* 2003*b*). Additionally during synaptic blockade, sDBS could directly alter firing thresholds and rates, but was unable to induce neuronal firing.

Methods

Thalamic slice preparation

Thalamic slices were prepared from 28 Sprague-Dawley rats (180–250 g) decapitated under halothane anaesthesia. All experiments were conducted using a protocol in accordance with the guidelines set out by the Canadian Council on Animal Care and were approved by the University of Calgary Animal Care Committee. Coronal sections (350–400 μm) were cut on a Vibratome (Leica VT 1000S) in cold oxygenated slicing medium consisting of (mM): 25 NaCl, 2.5 KCl, 4 $MgCl_2$, 1 $CaCl_2$, 1.2 NaH_2PO_4, 18 $NaHCO_3$, 200 sucrose. They were allowed to stabilize for 1–3 h in a holding chamber containing artificial cerebrospinal fluid (aCSF) consisting of (mM): 126 NaCl, 2.5 KCl, 1.2 $MgCl_2$, 2.4 $CaCl_2$, 1.2 NaH_2PO_4, 18 $NaHCO_3$, 11 glucose. Slices were then transferred to a recording chamber and superfused at 32°C with modified aCSF consisting of (mM): 126 NaCl, 2.5 KCl, 1.2 $MgCl_2$, 3.4 $CaCl_2$, 1.2 NaH_2PO_4, 18 $NaHCO_3$, 11 glucose.

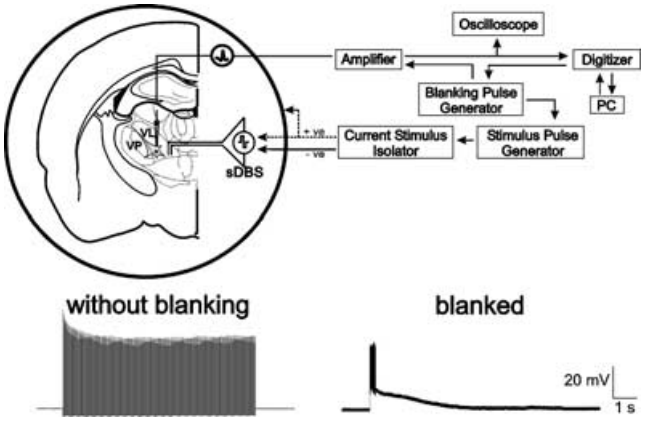

Figure 1. Experimental methods
Top: schematic representation of sharp intracellular recording set-up in thalamic rat brain slice. Note the two methods of stimulation using either the intranuclear bipolar electrode or the surrounding 'monopolar-ring' configuration. Recording and stimulation sites were in ventral-lateral (VL) or ventral-posterior (VP) nuclei. Bottom: intracellular recordings from the same cell with, and without the blanking operation activated.

Electrophysiological recordings

An Axoclamp-2A amplifier (Axon Instruments, CA, USA) was used in current-clamp mode for all experiments. Transmembrane current pulses were driven and captured using an A–D interface operated by pCLAMP software (Axon Instruments). The ventral thalamus was visually identified (Paxinos & Watson, 1998) and passive chart recordings of membrane response were digitized and recorded at 20 kHz using a CED micro 1401 (Cambridge Electronic Design, Cambridge, UK) controlled by Spike2 software.

Intracellular recordings were obtained using glass electrodes pulled from borosilicate glass (1.5 mm o.d., 0.86 mm i.d., AM Systems), filled with 4 M potassium acetate, 0.15 M KCl and having a final resistance of 75–120 MΩ. In some electrodes 2% neurobiotin (Vector Laboratories, CA, USA) was added to the intracellular solution for subsequent visualization of the recorded cells. All intracellular solutions were balanced to pH 7.4 using KOH or HCl as required. Input resistance was measured as the slope of the linear portion of the *I–V* curve, and is reported as the mean ± standard error of the mean (S.E.M.). For measuring input resistance during sDBS, intracellular direct current (DC) was manually injected to offset the depolarization induced by extracellular sDBS. A series of current steps were then administered to obtain the *I–V* curve plot and the slope resistance. To compare changes in postsynaptic excitability, current pulses and slow ramp current (−1.0 to 1.0 nA/2 s) were injected in control and during sDBS states.

Stimulation parameters, current spread and 'blanking' operation

A bipolar, tungsten stimulating electrode (0.1 mm diameter, 0.75 mm pole separation, 22–27 kΩ) was placed into the VL–VP thalamus for the delivery of the sDBS train (Fig. 1). In several experiments, stimulation was also delivered through a 'monopolar-ring' configuration, that is a monopolar stimulator with a circular bath ground as described by Garcia *et al.* (2003) (Fig. 1). Stimulation was delivered through a constant, isolated current source (A360 or A365, World Precision Instruments, FL, USA) and consisted of 10 s trains, at 125 Hz, of mono- or biphasic 60 μs square pulses of varying intensity (mean = 3.63 ± 2.77 mA, range = 0.5–10 mA).

Stimulation applied in a submerged recording chamber places the exposed portion of the stimulating electrode in contact with the tissue as well as the bath. This introduces a bath resistance in parallel with the tissue resistance.

© The Physiological Society 2004

Thus, given a bath resistivity of ∼50 Ω cm and a tissue resistivity of ∼500 Ω cm, the current seen by the tissue is less than 10% of that applied (Nowak & Bullier, 1996; McIntyre & Grill, 2002). Whereas we routinely report the current intensity applied, in this series of experiments the real tissue current was closer to an average of 327 μA. The resulting current density was 1–100 mA cm^{-2} (based on 90–900 μA applied current/surface area of electrode of 0.32 mm^2). This initial current is expected to drop off rapidly (McIntyre & Grill, 2001) and is estimated to be 2.58 mA cm^{-2} at 200 μm, 0.52 mA cm^{-2} at 500 μm and 0.31 mA cm^{-2} at 1000 μm away from the cathode. Thus, given a VL–VP thalamus of ∼2 mm^2 (Paxinos & Watson, 1998), the current level outside of this area would be very low and consequently the current spread was mainly limited to the VL–VP thalamus.

The high frequency stimulation used for sDBS produces an artifact that normally precludes the recording of membrane responses. To eliminate the stimulation artifact evoked during an sDBS train we applied brief (0.05–1 ms) blanking pulses that were triggered with each stimulus pulse (A-M Systems 2100, WA, USA). These voltage pulses were then used to initiate a blanking operation of the Axoclamp-2A amplifier, which prevented the membrane voltage from updating during the blanking pulse, thus significantly reducing the stimulus artifacts (Axon Instruments: Axoclamp-2A Operating Manual). Because of its short duration the blanking pulses did not significantly affect the latency and waveform of the evoked responses by sDBS. An example of stimulation with and without blanking is seen in Fig. 1.

Stimulation sites

The anatomical border between the VL and VP thalamus is nearly indistinguishable in the slice preparation (Paxinos & Watson, 1998), making exact determination of the recording site at the border region difficult. However, our recordings were in either VL or VP, and the type of membrane response induced by sDBS was not affected by the stimulation or recording site within these two nuclei. Similar responses (described in Results) were obtained from different recording sites within the VP–VL using a common stimulus location.

Experimental solutions

Kynurenate (KYN), 2-amino-5-phosphonovaleric acid (AP-V), 6,7-dinitroquinoxaline-2,3-dione (DNQX), picrotoxin and tetrodotoxin (TTX) (Sigma-Aldrich, MO, USA) were prepared as stock solution and bath applied at concentrations indicated in the Results. For blocking high-threshold Ca^{2+} conductances, equimolar concentrations of NaH_2PO_4 were replaced with NaCl, and 200 μM $CdSO_4$ (Fisher Scientific, TX, USA).

Neurobiotin labelling

To label recorded cells, neurobiotin was applied into cells by passing depolarizing intracellular pulses at 3 Hz with a current sufficient to produce action potentials on each pulse (0.2–2.0 nA) for 5–15 min. The slice was then fixed by immersion in a 4% paraformaldehyde, 4% sucrose solution in phosphate buffered saline (PBS) overnight. After several rinses in PBS, slices were sectioned at 60 μm using a cryostat, mounted onto slides and washed in a 0.1% Triton X-100, 0.2% BSA in PBS solution for 30 min. The slides were then incubated in avidin–fluorescein isothiocyanate (FITC) mixed in the Triton–BSA–PBS solution for 2 h and visualized with confocal microscopy.

Data analysis

Data are presented as means ± standard deviation (S.D.) except where otherwise noted. Statistical significance was tested with one-way ANOVA or Student's t test. Non-parametric data was analysed using the Kruskal-Wallis one-way ANOVA on ranks.

Results

Sixty-seven neurones from the VL–VP thalamus were studied all of which exhibited a low threshold Ca^{2+} spike (LTS) (Jahnsen & Llinas, 1984) and resting membrane potential of < -55 mV. Unless otherwise stated, no holding current was used during intracellular recordings. Despite repetitive high frequency stimuli, sDBS responses could be repetitively evoked in the same cell, or in multiple cells recorded from the same slice, suggesting a lack of stimulation-induced tissue damage. Intrathalamic sDBS induced a sustained membrane depolarization in 62 of 67 neurones recorded.

Subtypes of sDBS induced depolarization

The sDBS-induced depolarization was made up of two components: an initial transient depolarization from the resting membrane potential, followed by a sustained depolarization. The initial membrane depolarization was observed in all neurones and was characterized by a burst of action potentials. For calculation of the mean level of sustained depolarization, the membrane potential was measured at the 3, 5 and 7 s time mark of the sDBS train, and averaged. Based upon the amplitude of the sustained depolarization the sDBS-evoked responses could be divided into two categories. Type 1 responses ($n = 43$) quickly reached a depolarization plateau and began rapidly repolarizing within 1 s from the initial depolarization, resulting in a moderate sustained depolarization of 8.2 ± 6.1 mV and no further spike activity (Fig. 2*Aa*). In

© The Physiological Society 2004

contrast, type 2 responses ($n = 19$) did not appreciably repolarize and maintained a significantly larger plateau response (28.8 ± 8.3 mV; $P < 0.001$) over the entire course of stimulation. Following stimulation, the time to repolarization to baseline was variable, but recovery occurred within 30 s (Fig. 2*Ba*). The amplitude of the transient depolarization varied between the two types reaching 25.7 ± 8.9 mV (type 1) and 36.3 ± 11.35 mV (type 2) as measured during the interspike region ($P < 0.001$). Closer examination of the initial membrane

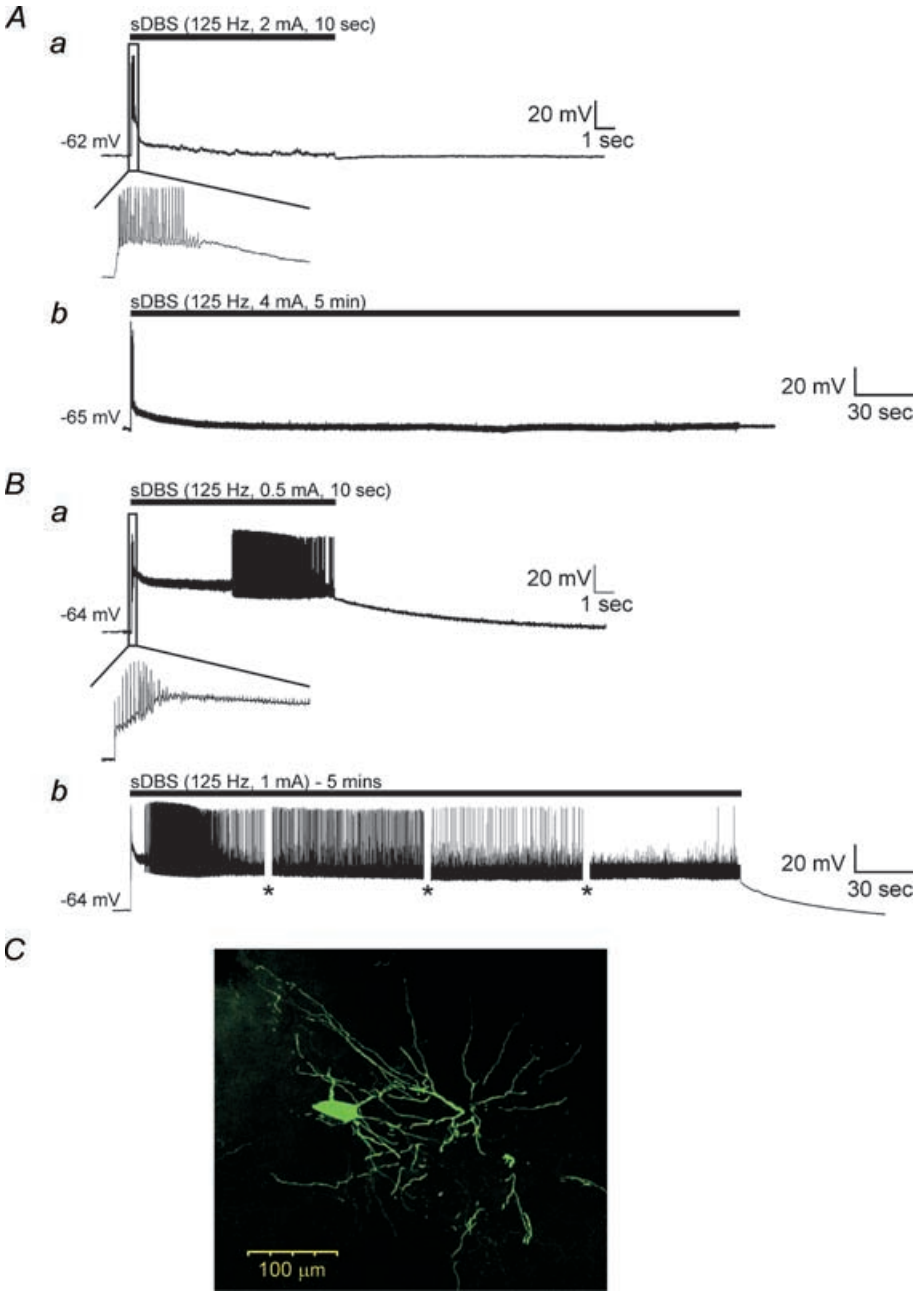

Figure 2. sDBS evoked two distinct types of membrane responses in ventral thalamic neurones
A, type 1 responses had a large initial depolarization declining toward a smaller but sustained level of depolarization in response to 10 s (*a*) or 5 min (*b*) of sDBS. The black bar indicates stimulus onset and duration. *B*, type 2 responses have a large initial depolarization, which persisted over 10 s (*a*) or 5 min (*b*) and led to varied spike activity. The insets show expanded initial responses during the 10 s sDBS train. The amplitude of action potentials in this and following figures were partially reduced due to digitization and some were also truncated or flattened by 'blanking pulses'. Gaps in the recording (shown as *) indicate times at which current pulse protocols were run during the 5 min sDBS train. *C*, morphology of a representative ventral thalamic neurone filled with neurobiotin. Note the extensive dendritic tree with numerous distal arborizations.

© The Physiological Society 2004

response revealed that the higher level of sustained depolarization observed in type 2 neurones often led to either spike inactivation or random high-frequency discharges that were absent in type 1 responses. While *in vivo* ventral thalamic cells are spontaneously active, *in vitro* they are not, owing in part to the reduced afferent synaptic input in slices (Contreras & Steriade, 1995; Steriade *et al.* 1996). As such, no firing was observed during repolarization to baseline following the cessation of stimulation with either response type.

Increasing the stimulation time to 5 ($n = 14$) or 10 min ($n = 9$) continued to induce similar sDBS membrane responses. In type 1 responses ($n = 11$) the sustained depolarization slowly decreased over the course of stimulation levelling off by 3 min at near baseline levels (1.42 ± 2.1 mV) (Fig. 2*Ab*). In type 2 responses ($n = 3$) the sustained depolarization remained elevated throughout stimulation although decreasing from 26.3 ± 4.5 mV at 10 s to 15.9 ± 3.7 mV at 5 min (Fig. 2*Bb*). Given that the rat ventral thalamus is composed of a homogeneous cell population (Williams & Faull, 1987; Ohara & Lieberman, 1993), it suggests that the two responses induced by sDBS occur in the same cell type. In line with this argument all recorded cells had similar resting membrane potentials (type 1, -65.2 ± 3.3 mV; type 2, -64.5 ± 3.1 mV) and steady-state input resistances (type 1, 54.1 ± 5.7 MΩ; type 2, 52.4 ± 5.3 MΩ). Neurones with both response types were filled with neurobiotin, and displayed typical morphology of thalamocortical relay cells characterized by an oval-shaped soma with bushy dendritic tree (Fig. 2*C*; $n = 4$). Furthermore, both response types could be observed in the same slice and there was no relationship between response type, current level or distance from the stimulating electrode (0.2–1.0 mm). Altering the current amplitude could not convert a type 1 to a type 2 membrane response. Finally, no difference was observed within the membrane response recorded from both the VL and VP nuclei.

sDBS-induced depolarizations are primarily mediated by glutamate

The influence of pharmacological blockade on sDBS-induced depolarization was tested in both membrane response types. Since the two types of sDBS-induced depolarizations showed identical sensitivity they are reported together.

We first tested whether the induction of sDBS-evoked depolarization requires action potential generation and intact synaptic transmission. We bath applied the Na^+ channel blocker TTX (0.1 μM) and monitored generation of action potentials triggered by current injection. In 7 out of 7 cells tested ($n = 4$ type 1, $n = 3$ type 2), TTX significantly reduced the initial depolarization (from 38.9 ± 10.2 mV to 7.1 ± 5.1 mV, $P < 0.05$) and the mean sustained depolarization (from 20.3 ± 10.6 mV to 1.1 ± 0.5 mV, $P < 0.05$). This occurred after the cell ceased to display action potentials indicating adequate blockade by TTX. Recovery of sDBS responses was obtained after TTX washout (37.7 ± 8.7 mV initial, 10.0 ± 4.9 mV sustained) (Fig. 3*A*).

The excitatory synaptic innervations in VL thalamus are predominantly provided by corticothalamic glutamatergic fibres (Deschênes & Hu, 1990). To examine the role of glutamate, we applied sDBS in the presence of kynurenate (KYN), a non-specific antagonist of ionotropic glutamate receptors. In 10 out of 10 cells tested ($n = 6$ type 1, $n = 4$ type 2), KYN (2 mM) reversibly reduced the initial depolarization from 29.4 ± 6.8 mV to 5.8 ± 3.7 mV ($P < 0.05$), and reduced the mean sustained depolarization from 15.9 ± 9.2 mV to 3.7 ± 4.5 mV ($P < 0.05$). KYN at this concentration also completely blocked the membrane depolarization evoked by exogenously applied AMPA (5 μM; $n = 3$), suggesting adequate blockade of postsynaptic glutamate receptors. Furthermore, in an additional six neurones ($n = 3$ type 1, $n = 3$ type 2), we bath applied a mixture of the NMDA receptor blocker AP-V (100 μM) and the non-NMDA antagonist DNQX (10 μM), during sDBS. We found these specific blockers of ionotropic glutamate receptors were equally effective in blocking sDBS-induced depolarizations (39.2 ± 12.2 mV to 4.4 ± 2.6 mV for initial depolarization and 18.6 ± 16.1 mV to 1.7 ± 1.7 mV for mean sustained; $P < 0.05$) (Fig. 3*B*).

In the next series of experiments, we tested whether blockade of voltage-dependent Ca^{2+} channels affected sDBS-induced depolarization. In 6 out of 6 neurones tested ($n = 4$ type 1, $n = 2$ type 2), bath application of Cd^{2+} (200 μM) reversibly inhibited both the initial depolarization (29.2 ± 7.1 mV to 4.4 ± 2.4 mV; $P < 0.05$) and the mean sustained response (20.1 ± 9.9 mV to 3.7 ± 2.4 mV; $P < 0.05$) (Fig. 4*A*). EPSPs induced by sDBS were highly sensitive to this concentration of Cd^{2+}; however, it did not affect the steady-state input resistance, Na^+-dependent action potentials, or the low threshold spikes (LTS) evoked by rebound from hyperpolarizing current injection (Figs 4*B* and *C*). Therefore, the blockade of sDBS by Cd^{2+} appears to be primarily mediated through presynaptic Ca^{2+} channels. During all pharmacological treatments, increasing the sDBS current to suprathreshold levels (up to 10 mA) failed to depolarize the cell further.

Finally, we tested the effects of the $GABA_A$ receptor antagonist picrotoxin (50 μM) on sDBS-induced depolarization ($n = 3$ type 1, $n = 1$ type 2). In all trials, picrotoxin failed to alter the induced depolarization or the response type. Furthermore, in control experiments it was not possible to evoke a unitary IPSP, nor was

© The Physiological Society 2004

there evidence of a mixed EPSP/IPSP ($n = 16$ of 16). Testing during glutamate receptor blockade failed to unmask an underlying IPSP, thereby suggesting a lack of significant GABAergic activation ($n = 5$, data not shown). Pharmacological data from all treatments are summarized in Fig. 5.

Non-synaptic effects of sDBS

Several recent studies reported that sDBS may directly modulate the excitability and firing pattern of individual neurones even after glutamatergic receptors are blocked (Beurrier *et al.* 2001; Magarinos-Ascone *et al.* 2002; Garcia *et al.* 2003). To test this possibility a series of hyper- and depolarizing current steps were administered in control and during sDBS in cells of both response types (Fig. 6). While there was no significant change in the steady-state input resistance as measured before (55.0 ± 7.6 MΩ) and during sDBS (54.3 ± 7.7 MΩ) ($n = 12$), alterations in transient currents were observed. Furthermore, the input resistance was similarly measured during application of kynurenate (2 mM, $n = 5$) in control and during sDBS conditions (Fig. 7*A*). Again there was no significant change in the input resistance between KYN trials, or in comparison to control (Fig. 7*B*). A visual examination of the voltage response to the current steps reveals an increase in firing rate during sDBS, and KYN + sDBS (Fig. 7*A*).

We next examined the neuronal membrane excitability before, and during sDBS using a slow ramp protocol that consisted of a series of 2 s current ramps (−1.0 to 1.0 nA). During sDBS, cell membrane potential was returned to baseline via direct current injection before each ramp was applied. As shown in Fig. 8*Aa* and *Ba*, during the control ramp, LTS and action potentials occurred at different potentials. During sDBS, while the threshold of LTS remained unchanged, action potentials occurred at a more negative membrane voltage ($P < 0.05$), suggesting a decrease in firing threshold. In type 1 responses ($n = 7$) the initial membrane voltage that triggered action potentials was lowered from -16.4 ± 12.5 mV to -21.6 ± 10.7 mV (Fig. 8*Ab*) and in type 2 responses ($n = 4$) it was lowered from -18.1 ± 13.4 mV to -29.0 ± 8.9 mV (Fig. 8*Bb*; $n = 4$). This alteration in firing threshold was not accompanied by a significant change in slope of the ramp, or apparent input resistance. The abnormally high membrane voltage

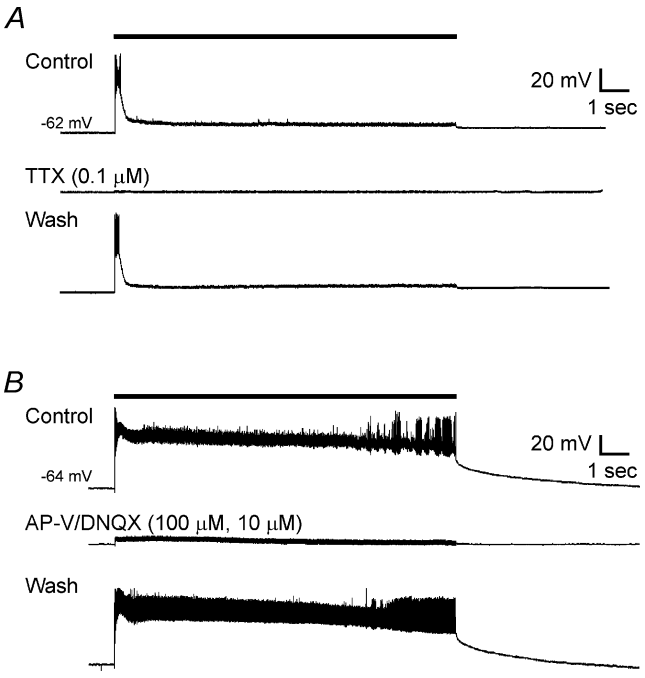

Figure 3. Pharmacological blockade of membrane responses induced by sDBS
Glutamate receptor (kynurenate, or AP-V–DNQX) or Na^+ channel (TTX) blockade were equally effective in preventing type 1 and 2 responses. *A*, type 1 response before, during and after washout of TTX. *B*, type 2 response to sDBS before, during and after washout of bath application of AP-V–DNQX. Note that glutamatergic blockade also eliminated action potentials induced by sDBS.

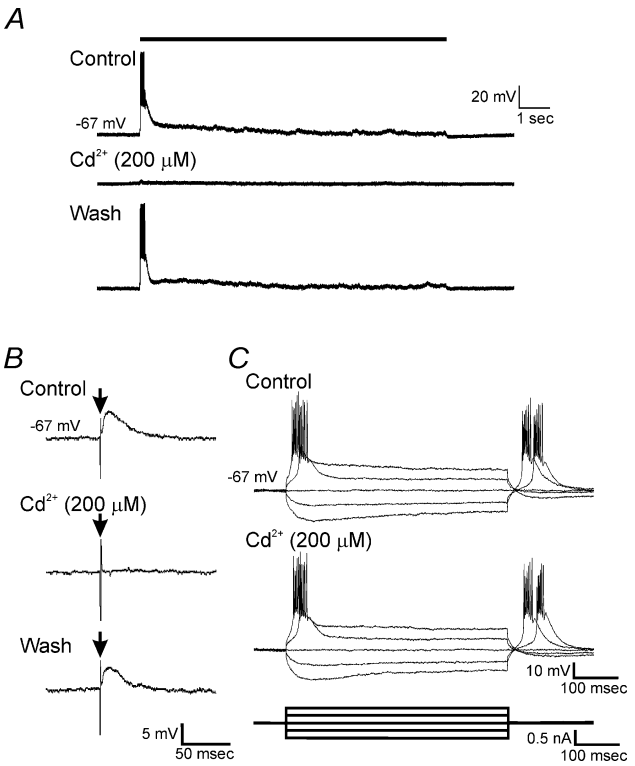

Figure 4. Cd^{2+} selectively blocked sDBS responses
A, membrane responses to sDBS before, during bath application of Cd^{2+}, and after washout. *B*, representative trace of single shock-evoked EPSPs before, during bath application of 200 μM Cd^{2+}, and after washout. Vertical excursion, indicated by arrow (↓), is stimulus artifact. *C*, current injection pulses recorded before and during bath application of 200 μM Cd^{2+}. Note that the T-type Ca^{2+} channel-dependent LTS remains unchanged in the presence of 200 μM Cd^{2+}. All recordings were obtained from the same cell.

© The Physiological Society 2004

for Na^+-dependent action potential firing is largely due to Na^+ channel inactivation during the slow ramp. This was required to slow membrane depolarization sufficiently to separate the low threshold Ca^{2+} spikes from the high threshold Na^+ action potentials.

The apparent change in membrane excitability was further supported by two additional series of experiments. First, ventral thalamic neurones exhibited a stimulation strength-dependent increase in firing rate during the ramp test (Fig. 9*A*, $n = 5$). This increase in firing rate was maintained in the presence of KYN (Fig. 9*B*, $n = 2$). In the second series of experiments, a series of brief intracellular pulses of varied intensity (3.3 Hz, 100 ms, 50–1000 pA) was applied in type 1 neurones after they had recovered to near baseline. Again intracellular current was manually injected to offset any remaining membrane depolarization. The total number of action potentials per series of 30 intracellular pulses was examined. The presence of single action potentials prevented the use of interspike interval as a measure of frequency. During sDBS the probability of firing was significantly enhanced by as much as 30.2%, indicating a significant increase over control ($P < 0.05$) (Fig. 10*A*). Similar to the firing probability, there was also a statistically significant increase in the firing frequency ($P < 0.05$) (Fig. 10*B*). The high level of sustained depolarization in type 2 responses prevented similar testing.

Stimulating electrode configuration

Recent reports in the subthalamic nucleus using 'monopolar-ring' stimulation (Garcia *et al.* 2003) have suggested that the effects of sDBS are *not* mediated by presynaptic neurotransmitter release, but rely on direct current activation. To examine this issue in our preparation we compared the sDBS response induced by bipolar or by the 'monopolar-ring' stimulation. For 'monopolar-ring'

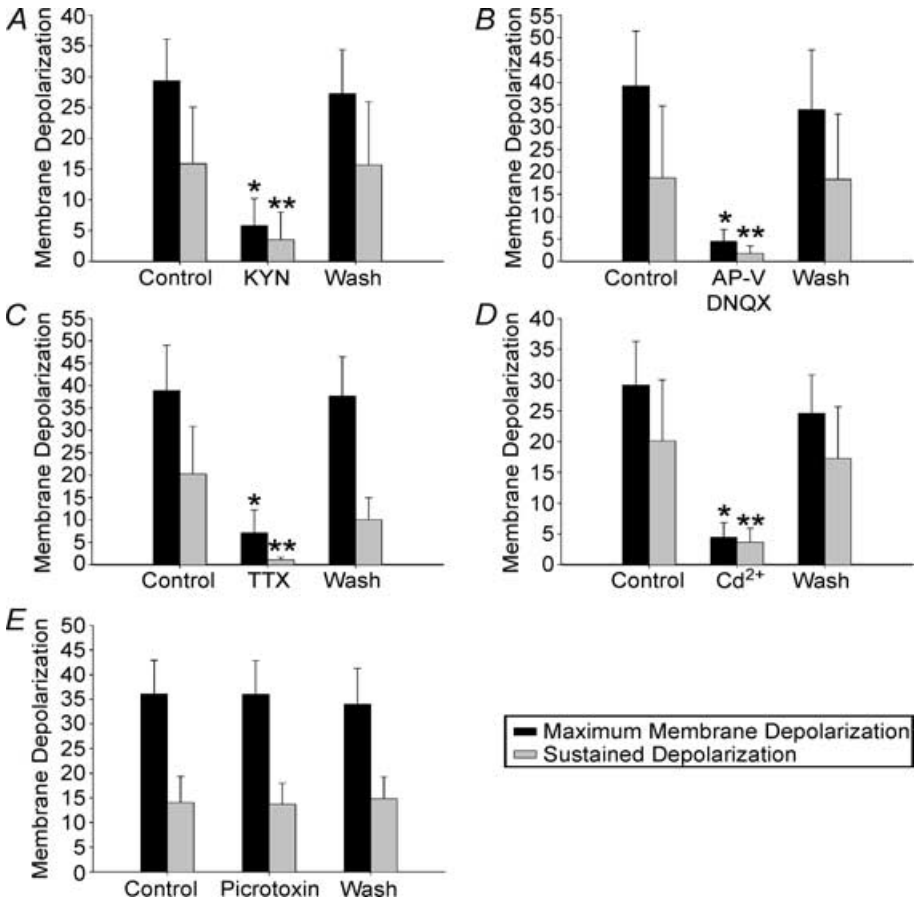

Figure 5. Summarized pharmacological data showing blockade of sDBS-induced maximal and sustained depolarization

Depolarization is almost eliminated in the presence of: kynurenate (2 mM; $n = 10$; *A*), AP-V–DNQX (100 μM–10 μM; $n = 6$; *B*), TTX (0.1 μM; $n = 7$; *C*), Cd^{2+} (200 μM; $n = 6$; *D*). Picrotoxin (50 μM; $n = 4$; *E*) does not affect membrane depolarization. Because both type 1 and 2 responding cells had similar suppression of depolarization, all data are presented together. Responses under pharmacological treatment that were statistically different from their respective control and washout values are indicated (* initial depolarization, ** mean sustained depolarization, $P < 0.05$).

© The Physiological Society 2004

stimulation one pole of the bipolar stimulator was used in conjunction with a round circular ground surrounding the tissue (Fig. 1). While the bipolar stimulator produced a large sDBS depolarization, 'monopolar-ring' stimulation, at the same current strength, failed to induce a characteristic sDBS response ($n = 15$). The 'monopolar-ring' stimulation produced minimal transient membrane depolarization of 5.9 ± 4.5 mV and sustained depolarization of 2.1 ± 2.7 mV. Increasing the current level to 3–5 times that used with the bipolar electrode elicited a characteristic sDBS response.

Discussion

Sustained high frequency intrathalamic stimulation alleviates tremor in patients with parkinsonian and essential tremor (Benabid *et al.* 1996). We have previously shown that sDBS in rat thalamic slices induces membrane depolarization that is stimulation frequency and amplitude dependent (Kiss *et al.* 2002). The results reported here indicate that the sDBS-induced depolarization in ventral thalamus is primarily of synaptic origin. It requires Ca^{2+}-dependent release of glutamate and activation of postsynaptic ionotropic glutamate receptors, thus demonstrating an obligatory role of synapses in mediating the thalamic depolarization in response to DBS. Independent of this depolarization, sDBS also has an important non-synaptic mechanism through a direct current effect that alters the evoked firing probability and frequency.

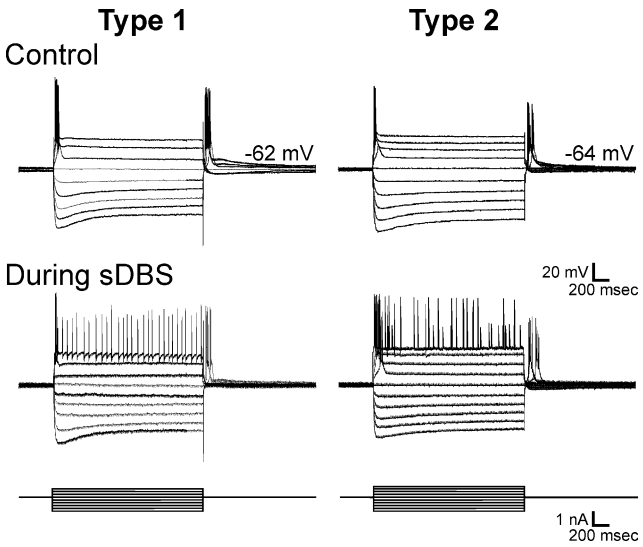

Figure 6. Effects of transmembrane current pulses
A, intracellular transmembrane current pulses (1 s) were applied to neurones previously identified as having a type 1 ($n = 8$) or type 2 ($n = 3$) membrane response to sDBS. Identical current pulses were re-applied during sDBS. Manual current was injected to offset the depolarization induced by sDBS. Note the similarity to transmembrane current pulse responses in both type 1 and 2 responding neurones, indicative of a common cell type.

sDBS-induced depolarization

In response to thalamic sDBS we observed two distinct membrane response types, characterized by an initial and varied sustained depolarization. As in our previous report (Kiss *et al.* 2002), sDBS response types were independent of stimulus strength and distance from the stimulating electrode. Furthermore, increasing the stimulation duration, up to 10 min, failed to change or reveal any additional response types. Both response types were equally sensitive to pharmacological blockade of action potentials, high-voltage Ca^{2+} channels, or glutamate receptors thereby demonstrating their dependence on synaptically released glutamate.

Two types of membrane responses

Both response types were equally distributed within the VL–VP thalamus, with type 1 responses observed in 69% of recordings, and type 2 in 31%. Following the initial depolarization and action potential burst of type 1 responses, the cells appeared quiescent for the remainder of the stimulus train. Furthermore, there appeared to be a significant degree of synaptic failure as there was no generation of EPSPs or partial spikes during the stimulation. This apparent 'functional deafferentation' may result from the blockade of afferent transmission, neurotransmitter depletion, postsynaptic desensitization and/or receptor trafficking. In contrast, in type 2 responses the initial depolarization induced by sDBS was larger, and was sustained throughout stimulation. In most cells a period of spike inactivation occurred following this initial depolarization. By increasing current intensity, the propensity and time course of this inactivation were also increased and lengthened. The sensitivity of this inactivation to current intensity and resultant membrane depolarization suggests it is mediated by Na^+ channel inactivation. Following this brief period of spike inactivation there was a varied degree of full and partial spike induction. These spikes may contribute to the increased 'noise' observed in type 2 over type 1 responses during sDBS (Figs 2 and 3).

Potential mechanism of the two membrane response types

The mechanism of the two types of membrane response to sDBS remains unknown. It is apparent, however, that both responses occur in the same cell types given that the cells displayed comparable input resistance, resting membrane potential, *I–V* curves, response to pharmacological

© The Physiological Society 2004

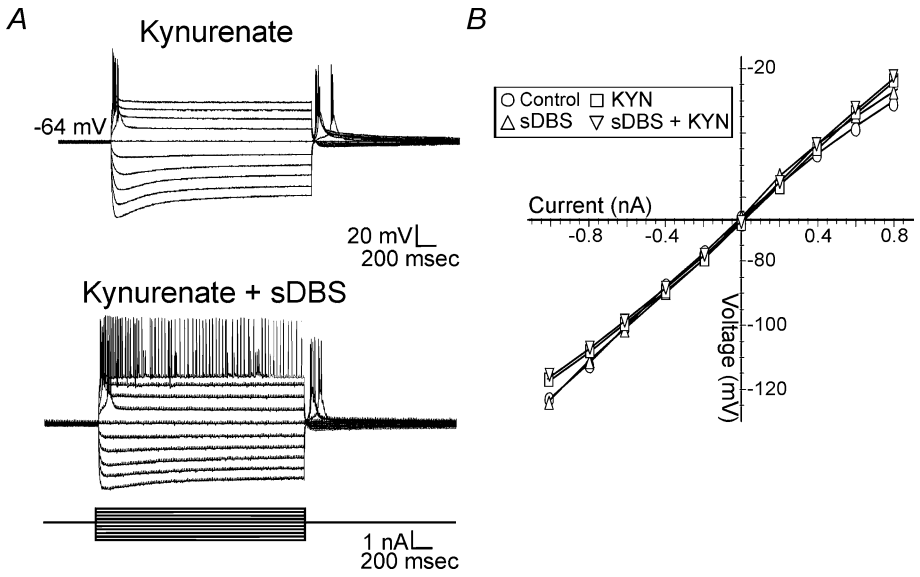

Figure 7. Effects of sDBS on membrane conductance
A, step current injections were used to obtain a *I–V* curve both during control sDBS or in the presence of kynurenate. Similar results were obtained for both type 1 and type 2 sDBS membrane responses. A representative trace from a type 2 response is displayed. *B*, no significant change in steady-state conductance during control (○), sDBS (Δ), kynurenate (□), or sDBS + kynurenate (∇). Each data point is derived from a minimum of 5 cells.

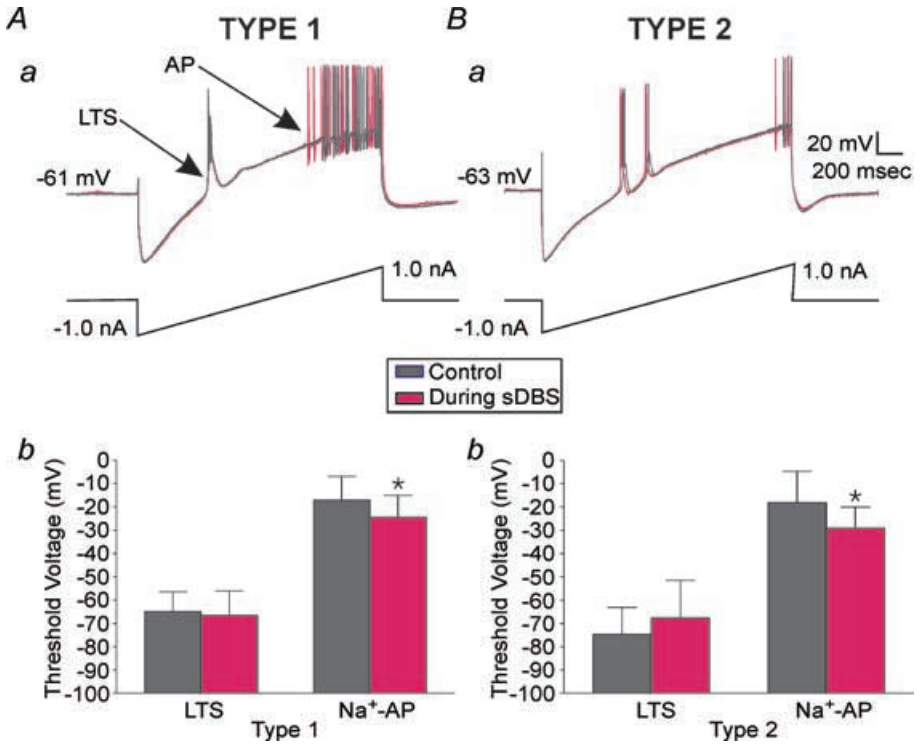

Figure 8. Decrease in firing threshold during sDBS
Overlayed recordings of membrane responses to ramp current injections (2 s, −1.0 to 1.0 nA) in type 1 (*Aa*) and type 2 (*Ba*) cells in control and during sDBS conditions. A significant decrease in the firing threshold for Na^+ spikes ($P < 0.05$) during sDBS but not in the low threshold Ca^{2+} spikes (LTS) was found with both response types. The summarized data are shown in *Ab* (type 1; $n = 7$) and *Bb* (type 2; $n = 4$).

© The Physiological Society 2004

manipulation and sensitivity to stimulation current level. Furthermore, while it was possible to record both response types from the same slice, even at the same distance from the stimulating electrode, it was not possible to convert between the two response types by increasing stimulation current, or applying the K^+ channel blocker 4-AP (data not shown).

Consequently, of critical importance may be variations in synaptic innervations and/or neurotransmitter release. Thalamic relay neurones issue extensive distal dendrites where numerous glutamatergic afferents from corticothalamic projections terminate (Guillery & Sherman, 2002). Selective innervation to different neurones may be responsible for the two membrane response types. It is known that specific regions of VL thalamus receive preferential synaptic contacts from different sources (Sato *et al.* 1997). Furthermore, composite EPSPs evoked by corticothalamic fibre stimulation in VL thalamus are about 5 times larger than those induced by cerebellar stimuli (Deschenes *et al.* 1984; Deschênes & Hu, 1990). Alternatively, neurotransmitter depletion may play an important role in type 1 *versus* type 2 responses. Thus, these two pathways may differ in their abilities to sustain the sDBS-evoked synaptic and glutamate-dependent depolarization. A better understanding of this issue requires detailed characterization of individual glutamatergic afferents to ventral thalamic neurones.

Beyond glutamatergic afferents, under *in vivo* physiological conditions the thalamus is inhibited via GABAergic input from the reticular thalamus and local interneurones. While in rat thalamus there is a relative lack of GABAergic interneurones, the synaptic terminals of the reticular nucleus remain intact in slices (Jones, 1985; Williams & Faull, 1987). As the $GABA_A$ receptor antagonist picrotoxin (50 μM) failed to alter or convert the membrane response to sDBS, GABAergic inhibition plays a minimal role in mediating the two membrane response types in the adult rat brain slice.

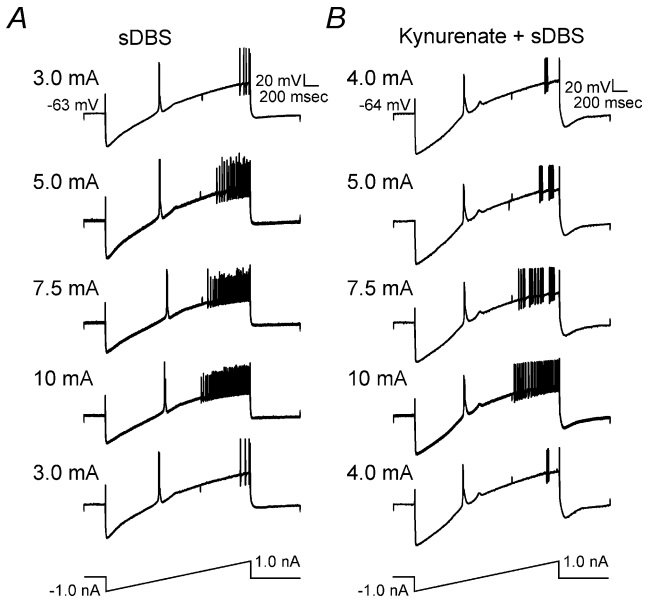

Figure 9. sDBS-induced increase in firing rate is dependent on stimulation strength, but independent of glutamate receptor activation

A, sDBS was applied at different intensities in the same type 1 neurone while spike firing rate was evaluated using ramp current injection. Increasing sDBS current amplitude significantly increased the firing rate. Note that comparable responses to ramp current injection were elicited in both *A* and *B* when initial sDBS current intensities were retested after high currents (up to 10 mA) were used. This indicates that no adverse membrane effect resulted from high sDBS current levels. *B*, the same firing rate tests as in*A* was applied in another neurone where glutamatergic transmission was blocked with 2 mM kynurenate.

Non-synaptic contributions

During sDBS Na^+-dependent action potentials increased in both frequency and firing probability. In contrast to the synaptic effects of sDBS, the change in firing rate was proportional to the level of sDBS current applied. Given the constant distance between stimulating and recording electrode, increasing the current applied will proportionally increase the current density at the recording electrode. This is similar to decreasing the distance from the stimulating electrode. Consequently, the non-synaptic effects are dependent upon distance. The increase in firing rate occurred independent of membrane depolarization as membrane potentials were manually clamped to resting levels. Furthermore, these sDBS-induced alterations were maintained during blockade of glutamate receptors thereby confirming their non-synaptic origin. The mechanism through which the non-synaptic effects of sDBS may alter the firing rate is unknown, but may reflect sDBS-induced alterations in the gating properties of the Na^+ channel related to changes in pH and/or Ca^{2+}-mediated charge screening (Cukierman *et al.* 1988; Zamponi & French, 1995; Tombaugh & Somjen, 1996; Boccaccio *et al.* 1998; Bruehl & Witte, 2003). In addition, while 80–95% of sDBS-induced somatic depolarization in our preparation was eliminated by effective pharmacological blockade of glutamatergic synaptic transmission, there remained a small residual membrane depolarization. This remaining residual membrane depolarization could derive from similar non-synaptic effects of sDBS such as electrotonic current flow and/or increased extracellular K^+ (Bikson *et al.* 2001; Lian *et al.* 2003). As these non-synaptic effects do not in and of themselves induce a significant depolarization or somatic action potentials, their contribution to the clinical mechanism of DBS in the thalamus appears limited. However in other tissues, such as the subthalamic nucleus, the relative contribution of these non-synaptic mechanisms may play a more important role.

© The Physiological Society 2004

Thalamic *versus* subthalamic DBS

In slices of the subthalamic nucleus (STN), sDBS has been shown to inhibit intrinsic membrane Na^+ currents (Beurrier *et al.* 2001; Magarinos-Ascone *et al.* 2002) and alter neuronal activity independent of synaptic activation (Garcia *et al.* 2003). Whereas this initially seems at odds with our data in ventral thalamus, the different results most likely reflect varying degrees of cell sensitivity to sDBS as well as the type and method of stimulation (see below). Indeed, Do & Bean (2003) have recently shown that high frequency stimulation in the STN produces slow inactivation of resurgent, persistent and transient components of the Na^+ current which dramatically alter the firing properties of cells. A resurgent Na^+ current has not been identified in thalamic cells and its apparent absence is indicative of how sDBS may have varying effects depending on the stimulated tissue.

Stimulation methods

Another confounding factor is the different types of stimulating electrodes used in various studies. For instance, bipolar stimulation in the STN predominantly effects presynaptic glutamate release (Lee *et al.* 2003), while monopolar-ring stimulation at similar current levels suggests a non-synaptic mechanism (Garcia *et al.* 2003). Such varied sensitivity in activating synaptic or non-synaptic components may well be related to the method of stimulation. During testing with a 'monopolar-ring' stimulator, we found that there was a dramatic reduction in synaptic activation as compared with bipolar stimulation.

The second consideration is the current levels used. The therapeutic benefits of DBS in humans are observed with stimulation intensities normally between 1 and 4 V, provided through a 1 kΩ stimulating electrode (Kiss *et al.* 2003*b*). As such, the therapeutic current levels would be between 1 and 4 mA. The mean current levels used in our slice preparation would consequently fall in the upper portion of this range. We also expect a significant degree of shunting of stimulation current to occur in an open perfusion chamber used for slice recordings (refer to Methods). This may also explain the variance seen in the aforementioned STN studies, as while similar current intensities were utilized in both studies, the current shunting would be dramatically reduced in the interface chamber used by Lee *et al.* (2003) thereby effectively increasing the current seen by the tissue.

Functional implications

While the ability of thalamic DBS to inhibit tremor has been well documented, its mechanism has proved elusive. Several studies have shown that locally DBS has an inhibitory action (Boraud *et al.* 1996; Dostrovsky *et al.* 2002), while others have shown increased efferent outflow activating the projection nuclei (Windels *et al.* 2000; Perlmutter *et al.* 2002; Anderson *et al.* 2003*a*; Hashimoto *et al.* 2003; Maurice *et al.* 2003; Windels *et al.* 2003). However, the similarity of the clinical benefits observed with DBS mirror that seen from thalamotomy (Schuurman *et al.* 2000) suggesting that local suppression of activity may be sufficient to stop the pathophysiological tremor signal from originating and/or propagating. This 'functional inactivation' mechanism is also consistent with thalamic DBS and microinjection of the $GABA_A$ agonist muscimol both stopping tremor (Pahapill *et al.* 1999).

While it has been suggested that modulation of the efferent outflow may be the essential mechanism through

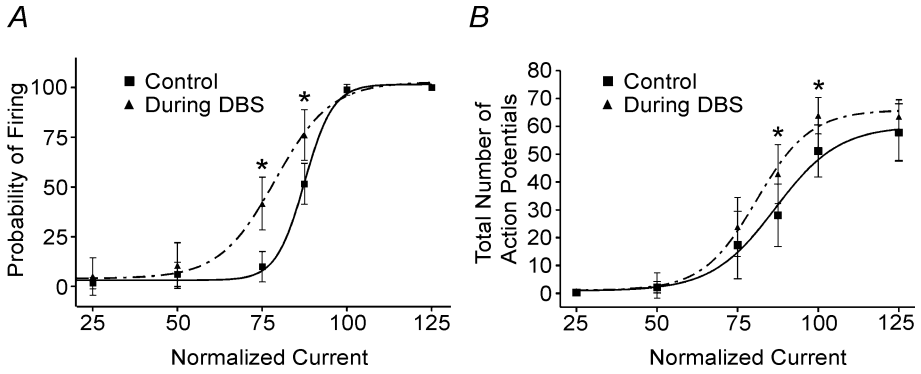

Figure 10. sDBS-induced increase in firing probability and frequency in a type 1 response
A train of 30 intracellular current pulses (3.3 Hz, 100 ms width) with varying intensities (50–1000 pA) were applied before (■) and during sDBS (▲). The firing probability and rate for each current level were calculated. Current was normalized to the intensity level that produced 100% probability of firing (see Results). The total number of action potentials per series of 30 intracellular pulses was examined. The presence of single action potentials prevented the use of interspike interval as a measure of frequency. Summarized data ($n = 3$ each) showing a significant increase in firing probability (*A*) and frequency (*B*) during sDBS are reported ($P < 0.05$).

© The Physiological Society 2004

which DBS exerts its clinical benefit (McIntyre *et al.* 2004) it is apparent that any mechanism (local or distant) which eliminates the propagation of the pathophysiological signal, would be equally effective. In this regard, we believe that the local effects of thalamic sDBS are mediated in two distinct ways. While both membrane response types show an initial burst of activity, type 1 responses quickly returned to baseline. During this period, there appeared to be complete synaptic failure as no additional EPSPs or partial spikes were observed. This 'functional deafferentation' may eliminate the pathological afferent signal that drives tremor cells (Lenz *et al.* 1994; Bergman & Deuschl, 2002), and thereby disrupt abnormal network activity. In type 2 responses, the sustained level of depolarization may through Na^+ channel inactivation, or depolarization-induced spike firing result in 'functional inactivation' or 'derhythmicity' (Benabid *et al.* 1996; Kiss *et al.* 2002) of the outgoing signal. Consequently, in both instances the network activity would be returned to a more functional state, eliminating the tremor signal propagation.

References

Anderson T, Hu B, Pittman Q & Kiss ZHT (2003*b*). Synaptic activation by deep brain stimulation: An intracellular study in rat thalamus. *Soc Neurosci Abstract* 185.4.

Anderson ME, Postupna N & Ruffo M (2003*a*). Effects of high-frequency stimulation in the internal globus pallidus on the activity of thalamic neurons in the awake monkey. *J Neurophysiol* **89**, 1150–1160.

Benabid AL, Pollak P, Gao DM, Hoffmann D, Limousin P, Gay E, Payen I & Benazzouz A (1996). Chronic electrical stimulation of the ventralis intermedius nucleus of the thalamus as a treatment of movement disorder. *J Neurosurg* **84**, 203–214.

Bergman H & Deuschl G (2002). Pathophysiology of Parkinson's disease: from clinical neurology to basic neuroscience and back. *Mov Disord* **17** (Suppl. 3), S28–S40.

Beurrier C, Bioulac B, Audin J & Hammond C (2001). High-frequency stimulation produces a transient blockade of voltage-gated currents in subthalamic neurons. *J Neurophysiol* **85**, 1351–1356.

Bikson M, Lian J, Hahn PJ, Stacey WC, Sciortino C & Durand DM (2001). Suppression of epileptiform activity by high frequency sinusoidal fields in rat hippocampal slices. *J Physiol* **531**, 181–191.

Boccaccio A, Moran O & Conti F (1998). Calcium dependent shifts of Na^+ channel activation correlated with the state dependence of calcium-binding to the pore. *Eur Biophys J* **27**, 558–566.

Boraud T, Bezard E, Bioulac B & Gross C (1996). High frequency stimulation of the internal globus pallidus (GPi) simultaneously improves parkinsonian symptoms and reduces the firing frequency of GPi neurons in the MPTP-treated monkey. *Neurosci Lett* **215**, 17–20.

Bruehl C & Witte OW (2003). Relation between bicarbonate concentration and voltage dependence of sodium currents in freshly isolated CA1 neurons of the rat. *J Neurophysiol* **89**, 2489–2498.

Contreras D & Steriade M (1995). Cellular basis of EEG slow rhythms: a study of dynamic corticothalamic relationships. *J Neurosci* **15**, 604–622.

Cukierman S, Zinkand WC, French RJ & Krueger BK (1988). Effects of membrane surface charge and calcium on the gating of rat brain sodium channels in planar bilayers. *J General Physiol* **92**, 431–447.

Deschênes M & Hu B (1990). Electrophysiology and pharmacology of corticothalamic input in neurons of the lateral thalamic nuclei: An intracellular study in the cat. *Eur J Neurosci* **2**, 140–152.

Deschenes M, Paradis M, Roy JP & Steriade M (1984). Electrophysiology of neurons of lateral thalamic nuclei in cat: resting properties and burst discharges. *J Neurophysiol* **51**, 1196–1219.

Do MT & Bean BP (2003). Subthreshold sodium currents and pacemaking of subthalamic neurons: modulation by slow inactivation. *Neuron* **39**, 109–120.

Dostrovsky JO, Levy R, Wu JP, Hutchison WD, Tasker RR & Lozano AM (2000). Microstimulation-induced inhibition of neuronal firing in human globus pallidus. *J Neurophysiol* **84**, 570–574.

Dostrovsky JO, Patra S, Hutchison WD, Palter VN, Filali M & Lozano AM (2002). Effects of stimulation in human thalamus on activity of nearby thalamic neurons. *Soc Neurosci Abstract* 62.14.

Garcia L, Audin J, D'Alessandro G, Bioulac B & Hammond C (2003). Dual effect of high-frequency stimulation on subthalamic neuron activity. *J Neurosci* **23**, 8743–8751.

Guillery RW & Sherman SM (2002). Thalamic relay functions and their role in corticocortical communication: generalizations from the visual system. *Neuron* **33**, 163–175.

Hashimoto T, Elder CM, Okun MS, Patrick SK & Vitek JL (2003). Stimulation of the subthalamic nucleus changes the firing pattern of pallidal neurons. *J Neurosci* **23**, 1916–1923.

Holsheimer J, Demeulemeester H, Nuttin B, & de Sutter P (2000). Identification of the target neuronal elements in electrical deep brain stimulation. *Eur J Neurosci* **12**, 4573–4577.

Jahnsen H & Llinas RR (1984). Electrophysiological properties of guinea-pig thalamic neurones: an in vitro study. *J Physiol* **349**, 205–226.

Jones EG (1985). *The Thalamus*. Plenum, New York.

Kiss ZHT, Anderson T, Hansen T, Kirstein DD, Suchowersky O & Hu B (2003*a*). Neural substrates of microstimulation-evoked tingling: a chronaxie study in human somatosensory thalamus. *Eur J Neurosci* **18**, 728–732.

Kiss ZHT, Mooney D, Renaud L & Hu B (2002). Neuronal response to local electrical stimulation in rat thalamus: Physiological implications for the mechanism of action of deep brain stimulation. *Neurosci* **113**, 137–143.

Kiss ZHT, Wilkinson M, Krcek J, Suchowersky O, Hu B, Murphy W, Hobson D & Tasker RR (2003*b*). Is the target for thalamic DBS the same as for thalamotomy? *Mov Disord* **18**, 1169–1175.

© The Physiological Society 2004

Lee KH, Roberts DW & Kim U (2003). Effect of high-frequency stimulation of the subthalamic nucleus on subthalamic neurons: An intracellular study. *Stereotact Funct Neurosurg* **80**, 32–36.

Lenz FA, Kwan HC, Martin RL, Tasker RR, Dostrovsky JO & Lenz YE (1994). Single unit analysis of the human ventral thalamic nuclear group: tremor-related activity in functionally identified cells. *Brain* **117**, 531–543.

Lian J, Bikson M, Sciortino C, Stacey WC & Durand DM (2003). Local suppression of epileptiform activity by electrical stimulation in rat hippocampus in vitro. *J Physiol* **547**, 427–434.

McIntyre CC & Grill WM (2001). Finite element analysis of the current-density and electric field generated by metal microelectrodes. *Ann Biomed Eng* **29**, 227–235.

McIntyre CC & Grill WM (2002). Extracellular stimulation of central neurons: Influence of stimulus waveform and frequency on neuronal output. *J Neurophysiol* **88**, 1592–1604.

McIntyre CC, Grill WM, Sherman DL & Thakor NV (2004). Cellular effects of deep brain stimulation: Model-based analysis of activation and inhibition. *J Neurophysiol* **91**, 1457–1469.

Magarinos-Ascone C, Pazo JH, Macadar O & Buno W (2002). High-frequency stimulation of the subthalamic nucleus silences subthalamic neurons: a possible cellular mechanism in Parkinson's disease. *Neurosci* **115**, 1109–1117.

Maurice N, Thierry AM, Glowinski J & Deniau JM (2003). Spontaneous and evoked activity of substantia nigra pars reticulata neurons during high-frequency stimulation of the subthalamic nucleus. *J Neurosci* **23**, 9929–9936.

Nowak LG & Bullier J (1996). Spread of stimulating current in the cortical grey matter of rat visual cortex studied on a new in vitro slice preparation. *J Neurosci Meth* **67**, 237–248.

Ohara PT & Lieberman AR (1993). Some aspects of the synaptic circuitry underlying inhibition in the ventrobasal thalamus. *J Neurocytol* **22**, 815–825.

Pahapill PA, Levy R, Dostrovsky JO, Davis KD, Rezai AR, Tasker RR & Lozano AM (1999). Tremor arrest with thalamic microinjections of muscimol in patients with essential tremor. *Ann Neurol* **46**, 249–252.

Paxinos G & Watson C (1998). *The Rat Brain in Stereotactic Coordinates*, 4th edn. Academic Press, San Diego.

Perlmutter JS, Mink JW, Bastian AJ, Zackowski K, Hershey T, Miyawaki E, Koller W & Videen TO (2002). Blood flow responses to deep brain stimulation of thalamus. *Neurology* **58**, 1388–1394.

Ranck JB (1975). Which elements are excited in electrical stimulation of mammalian central nervous system: a review. *Brain Res* **98**, 417–440.

Sato F, Nakamura Y & Shinoda Y (1997). Serial electron microscopic reconstruction of axon terminals on physiologically identified thalamocortical neurons in the cat ventral lateral nucleus. *J Comp Neurol* **388**, 613–631.

Schuurman PR, Bosch DA, Bossuyt PMM, Bonsel GJ, Van Someren EJW, Bie RM, Merkus MP & Speelman JD (2000). A comparison of continuous thalamic stimulation and thalamotomy for suppression of severe tremor. *N Engl J Med* **342**, 461–468.

Sommer MA (2003). The role of the thalamus in motor control. *Curr Opin Neurobiol* **13**, 663–670.

Stepniewska I, Sakai ST, Qi HX & Kaas JH (2003). Somatosensory input to the ventrolateral thalamic region in the macaque monkey: potential substrate for parkinsonian tremor. *J Comp Neurol* **455**, 378–395.

Steriade M, Contreras D, Amzica F & Timofeev I (1996). Synchronization of fast (30–40 Hz) spontaneous oscillations in intrathalamic and thalamocortical networks. *J Neurosci* **16**, 2788–2808.

Tombaugh GC & Somjen GG (1996). Effects of extracellular pH on voltage-gated Na^+, K^+ and Ca^{2+} currents in isolated rat CA1 neurons. *J Physiol* **493**, 719–732.

Vitek JL (2002). Mechanisms of deep brain stimulation: Excitation or inhibition. *Mov Disord* **17** (Suppl 3), S69–S72.

Williams MN & Faull RL (1987). The distribution and morphology of identified thalamocortical projection neurons and glial cells with reference to the question of interneurons in the ventrolateral nucleus of the rat thalamus. *Neurosci* **21**, 767–780.

Windels F, Bruet N, Poupard A, Feuerstein C, Bertrand A & Savasta M (2003). Influence of the frequency parameter on extracellular glutamate and gamma-aminobutyric acid in substantia nigra and globus pallidus during electrical stimulation of subthalamic nucleus in rats. *J Neurosci Res* **72**, 259–267.

Windels F, Bruet N, Poupard A, Urbain N, Chouvet G, Feuerstein C & Savasta M (2000). Effects of high frequency stimulation of subthalamic nucleus on extracellular glutamate and GABA in substantia nigra and globus pallidus in the normal rat. *Eur J Neurosci* **12**, 4141–4146.

Zamponi GW & French RJ (1995). Sodium current inhibition by internal calcium: a combination of open-channel block and surface charge screening? *J Membr Biol* **147**, 1–6.

Acknowledgements

Funding for this project was provided by the Alberta Heritage Foundation for Medical Research (AHFMR), Arthur Henry and Alice Elizabeth Zoe Fitzgerald Fund, the American Association of Neurological Surgeons, Banting Research Foundation and the Canadian Institutes of Health Research (CIHR). T.A. is a fellow of the Parkinson Society Canada, Q.P. is an AHFMR Medical Scientist, and Z.H.T.K. is a CIHR Clinician-Scientist and an AHFMR Clinician-Investigator.

© The Physiological Society 2004